

Study of Graphite DC ARC and the Structural Studies of Carbon Nanotubes Prepared in the DC ARC

Zuhoor Elahi*

Department of Physics, University of Karachi, Karachi, Pakistan

Research Article

Received: 10-Jun-2022, Manuscript No. JOMS-22-64667; **Editor assigned:** 13-Jun-2022, PreQC No. JOMS-22-64667(PQ); **Reviewed:** 27-Jun-2022, QC No. JOMS-22-64667; **Revised:** 05-Jul-2022, Manuscript No. JOMS-22-64667(R); **Published:** 13-Jul-2022, DOI: 10.4172/2321-6212.10.6.004.

***For Correspondence:**

Zuhoor Elahi, Department of Physics, University of Karachi, Karachi, Pakistan.

E-mail:

zuhoor.elahi@uok.edu.pk

Keywords: DC ARC; Carbon nanotubes; Excitation temperature; Electron density

ABSTRACT

A study of DC Arc plasma column during the preparation of carbon nanotubes is presented. Such study was planned to study the experimental parameters, which influence the formation of nano-structures. Excitation temperatures are measured by using the intensities of consecutive ionization states in the line spectrum. The dependence of excitation temperature on delay time is calculated and shown graphically. Electron densities are also calculated at different times in the arc plasma and are found to be decreasing exponentially as the plasma gets cool down. Carbon nanotubes that are formed during the arc are collected from the cathode in the form of soot and studied for morphology, composition, and structural properties. It is found that the nanotubes formed are of multiwalled nature.

INTRODUCTION

Nanotechnology has empowered the usage of nanoparticles with the size of under 100 nm in numerous applications. Researchers are consistently searching for innovative applications using nanoparticles. After the discovery of carbon nanotubes efforts have been committed to find effective methods for their synthesis [1]. However, there are usually not much publications in respect to the elementary methods that happen in the graphite

arc in which these structures grow. The examination of graphite arc plasma is essential to understand the creation and the decay of carbon molecules in a high-temperature area, which can be associated with the formation of carbon nanostructures. The optical emission spectroscopy appeared to be remarkably appropriate technique for these sorts of studies. Some fairly qualitative outcomes on the characteristics of carbon plasma in the production of carbon nanostructures have just been published. It is notable that the development of carbon nanotubes in a DC/AC arc between graphite terminals happens in a chaotic environment which is not easy to control on such a small scale. Be that as it may, on the large scale one can predict distinctive strategies for affecting the arc discharge, e.g. by the pressure, input voltage/current control, distance between the electrodes, the diameters of the electrodes, or by changing condensation rates by various cooling techniques^[1].

Carbon nanotubes can go about as a catalyst medium in a fuel cell and keeping away from the utilization of platinum which is much expensive, and most catalysts depend on. A few researchers have set up a strategy to develop integrated circuits utilizing carbon nanotubes ^[2]. Arc discharge was the first recognized procedure for producing Single-Walled Nano Tubes (SWNTs) ^[1,3] and Multi Walled Nano Tubes (MWNTs) ^[1,4]. used the graphite bars in contact by applying an AC voltage in a noble gas environment to create Bucky balls, while in the DC arc the positive anode is sublimated and creates fullerenes^[5] as ash in the chamber, and a small amount of the positive electrode is dissipated and stored on the negative electrode in the form of powder. In that cathode deposit, Iijima, in the year 1991, first observed the carbon nanotubes ^[1]. The yield for this approach is dependent upon 30% by weight. In this approach both SWNTs and MWNTs are formed with their lengths up to 50 micrometres ^[6].

MATERIALS AND METHODS

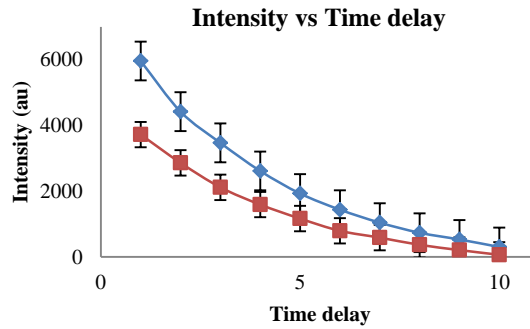
Experimental work

A small stainless-steel vacuum chamber is used for the formation of DC arc between the graphite electrodes. During the arc carbon nanotubes are formed. The deposition chamber consists of four major components; (1) the chamber, (2) sample holders, (3) optical window, (4) and Vacuum system. The temperature of the electrodes can be adjusted for different values of currents as it is an important factor which the properties of produced nanoparticles depend on. Optical studies of the arc during the formation of carbon nanotubes are carried out by Avantes spectrometer. Spectra are recorded during the arc by using the spectrometer setup which consists of a spectrometer attached through an optical fibre cable to a computer, and on the other side to the deposition chamber. The obtained spectra can be analysed to find temperature, density, etc. of the synthesized nanostructures. The nanostructures formed there are then also studied for their morphological, elemental and structural properties.

Characterization

The observed values of intensities are used to calculate excitation temperature and densities within plasma. The intensities of two lines as a function of delay time. Excitation temperatures and densities are found by using the Boltzmann plot method and Saha-Eggert equation respectively. Morphological, elemental, and structural studies are carried out by using SEM, EDX, and XRD techniques Figure 1.

Figure 1. The intensities of two spectral lines in emission spectrum of arc are plotted against time delay. Note: $\color{blue}\blacklozenge$ 11, $\color{red}\blacksquare$ 12



Excitation temperature measurement: The excitation temperatures are usually calculated with the help of relative intensities of the spectral lines in the emission spectrum using the Boltzmann equation given below [7]:

$$\ln \left[\frac{\lambda_{ki} I}{g_k A_{ki}} \right] = C - \frac{E_k}{k_B T} \dots\dots\dots (1)$$

The values A_{ki} , g_k , and E_k are obtained from the website of NIST database.

The excitation temperatures in the plasma arc can be found by using spectral lines in the emission spectrum of carbon. The Boltzmann function $\ln \left[\frac{\lambda_{ki} I}{g_k A_{ki}} \right]$ for different lines is calculated and plotted against the upper level energy E_k as shown in the Figure 2 and listed in the Table 1. The plot of Boltzmann function versus energy of upper level yields straight lines. The slopes (S) of these lines are $-1/k_B T$, assuming that there is a Boltzmann distribution in the populations. We can write:

$$k_B T = -\frac{1}{S} \dots\dots\dots \text{(in eV)} (2)$$

$$T = -\frac{1}{k_B S} \dots\dots\dots \text{(in K)} (3)$$

Figure 2. Boltzmann function $\ln[\lambda_{ki}I/g_k A_{ki}]$ is plotted against the upper level energy (in eV). Note: $\color{blue}\blacklozenge$ at 1 ms, $\color{red}\blacksquare$ at 2 ms, $\color{green}\blacktriangle$ at 3 ms, $\color{purple}\times$ at 4 ms, $\color{cyan}\blacklozenge$ at 5 ms

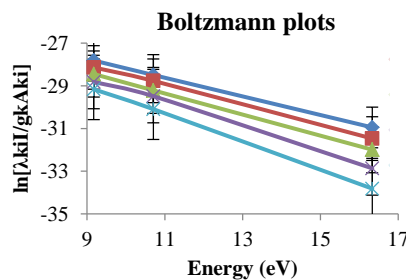


Table 1. The values of the transition probabilities, and the energies of upper levels for the carbon lines taken from the NIST database.

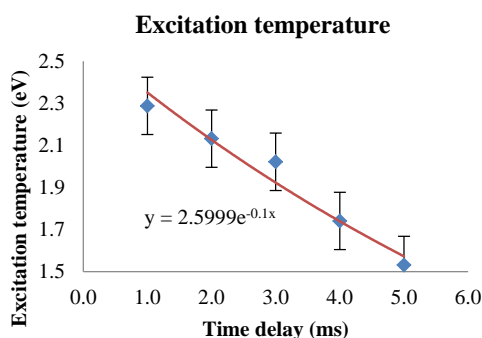
Wavelength λ (nm)	E_k (eV)	g_k	A_{ki} $\times 10^7$ /cm	$\lambda_{ki}/g_k A_{ki}$ $\times 10^{14}$	$\ln[\lambda_{ki}/g_k A_{ki}]$				
					at 0 ms	at 1 ms	at 2 ms	at 3 ms	at 4 ms
601.484	10.7	3	0.16	0.125	23.89	24.16	24.61	24.88	25.49
657.805	16.33	4	3.67	44.81	26.34	26.87	27.39	28.26	29.21
833.515	9.17	1	3.51	2.375	23.21	23.54	23.84	24.22	24.56

Table 2 shows the electrons temperatures obtained from the slopes of the straight lines of Figure 2. The measured values of excitation temperatures are plotted as function of delay time in the Figure 3.

Table 2. The temperature measurement by the slopes of the Boltzmann plots of Figure

Time delay (ms)	Slope, S (eV) ⁻¹	$k_B T = -1/S$ (eV)	T (K)
1	-0.437	2.288	26549.913
2	-0.469	2.132	24744.066
3	-0.495	2.022	23468.083
4	-0.574	1.741	20203.633
5	-0.653	1.532	17777.216

Figure 3. The excitation temperature calculated from the Boltzmann plot of Figure are plotted as function of time delay. Note: $\blacklozenge k_B T = -1/S$



Electron density measurement: Saha-Eggert relationship is used to determine the electron densities within plasma. The relative intensities of the neutral atomic lines and the singly charged ionic lines of carbon are used in this equation.

$$N_e = 4.83 \times 10^{15} \frac{I^0 g^+ A^+ \lambda^0}{I^+ g^0 A^0 \lambda^+} T^{3/2} \exp \left[\frac{E^+ + \Delta E_1 - E^0 - E_1}{k_B T} \right]$$

Figure 4 shows the plot of estimated values of electron densities versus delay time. The electron densities are also plotted against excitation temperatures in the Figure 5.

Figure 4. Electron density of plasma arc as calculated from the Saha-Eggert equation is plotted against the delay time. Note: ● Electron, — Expon

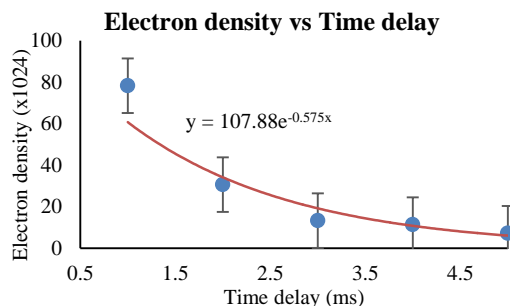
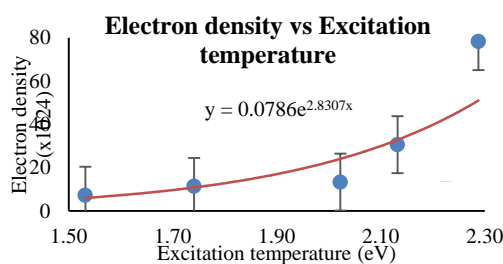


Figure 5. Dependence of the electron density on the excitation temperature. Note: ● Electron



Figures 4 and 5 show that the dependence of electron density on both the delay time, and excitation temperature is exponential.

Morphology: The synthesized carbon nanotubes are analyzed for surface morphology by using the SEM images. The SEM images of the samples are shown in the Figure 6 at different magnifications. Junks of carbon nanotubes can be seen in the Figure 6. It can also be seen that nanotubes formed are of large lengths and very small diameters.

Composition: The elemental analysis of the samples is carried out by taking EDX spectrum. Figure 7 shows the EDX spectrum of a sample. Purity index of the carbon nanotubes is clear in the spectrum. There are three peaks in the spectrum. The most intense peak appeared at ~ 3 eV confirms that there are only carbon atoms present in the samples. The carbon is about 71% by weight and oxygen. It also proves the high purity of the graphite rods that are used as the electrodes with the DC power supply for producing DC arc. The second peak is relatively very small which shows the presence of oxygen atoms in the samples. This is since the experiment is done in the air atmosphere. The third peak is of gold, which is since the samples are electroplated with, for the SEM studies.

Figure 6. SEM images of the samples at different magnifications showing nanotubes formed during the arc discharge. (a) at 40,000X, (b) at 30,000X.

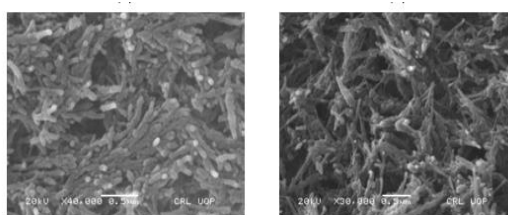
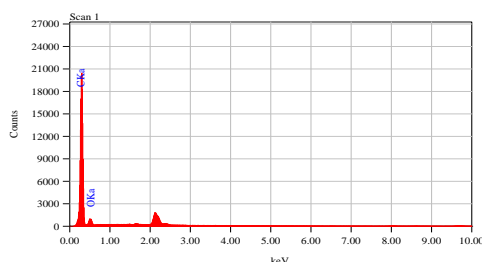
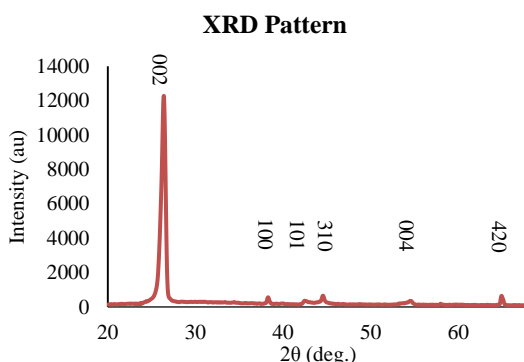


Figure 7. EDX spectrum of the sample.



Crystal structure: The XRD pattern of the sample is shown in the Figure 8 below. The diffraction peaks appeared in the XRD spectrum match very well with literature patterns. The most intense and the sharp reflection peak (002) appeared at 26.4° indicates the concentric cylindrical nature of graphene sheets nested together and that the nanotubes are multiwalled in nature [8,9].

Figure 8. XRD pattern of carbon nanotubes in which the intense peak at 26.40 shows the 002 reflection of the multiwalled carbon nanotubes. The other peaks at 42.40, 44.550, and 55° correspond to the 100, 101, and 004 reflections of the carbon atoms.



The presence of the peaks at 42.4° and 55° corresponding to the 100 reflection [10] and 004 reflection of carbon atoms respectively are also in good agreement with the literature [10,11].

Lattice constant : Lattice constants for different peaks are calculated by using the formula:

$$a = \frac{\lambda}{2 \sin \theta} \sqrt{h^2 + k^2 + l^2} \dots\dots\dots (1)$$

Average value of the lattice constants for the planes is found to be 6.602 Å.

Plane Spacing: The planes spacings d for all peaks are calculated by using the Bragg's law:

$$n\lambda = 2d \sin \theta \dots\dots\dots (7)$$

The calculated values of 'd' are listed in the Table 3. The most intense peak appeared at 26.4° in the XRD pattern confirms the presence of carbon nanotubes, and the plane of this peak is named as 002 in the literature [8,12,13]. The plane spacing at this peak is found to be 3.373 Å, which is also well matched with the literature for multi-walled carbon nanotubes (Tables 3 and 4) [14].

Table 3. The quantitative analysis: Fitting Coefficient: 0.9165.

Element	(keV)	mass%	Error%	At%	K
C K	0.277	68.64	1	74.46	76.56
O K	0.525	31.36	8.15	25.54	23.43
Total		100		100	

Table 4. Planes spacing for different peaks in XRD data of the carbon nanotubes are calculated by using the Bragg’s law.

S.No.	2θ (deg)	Intensity (I) (au)	I / I ₀ %	d-value (Å)
1	26.4	12278	100	3.373
2	38.25	540	4	2.352
3	42.4	345	3	2.13
4	44.55	655	5	2.032
5	64.9	641	5	1.436
6	69.3	236	2	1.355

RESULTS AND DISCUSSIONS

During the evaporation of graphite rods, a portion of the positive electrode is consumed. The rate of reduction in length of anode is measured to be 2 mm/s. Excitation temperatures are measured to be in the range of 20,000 to 30,000 kelvin that are in good agreement with reported values [15-19]. The electron densities in the arc plasma are measuring to be of the order of $\times 10^{24}$ particles. In Figure 4, the electron densities are falling exponentially with time which in turn implies that the electron densities are decreasing exponentially with the decrease in temperature within the plasma. The SEM images show that most of the particles have diameters ranging from approximately 5 to 30 nanometers, and their lengths are of the order of hundreds of nanometers.

The EDX spectrum of the samples show the purity index of carbon in the prepared samples, which is found to be ~ 71 weight% (Figure 7). The second peak is of oxygen which is since all the experiments are done in open air at atmospheric pressure. The third peak, which is not labeled, is of gold, because the samples are electroplated with gold for the SEM/ EDX analysis. The average value of the lattice constant is found to be 6.602 Å. The plane’s spacing for 002 peaks is calculated to be 3.373 Å by using Bragg’s law [20-26].

Also, the results are well matched with the literature patterns, according to which it is reported that the prepared nanostructures are multiwalled in nature [8].

CONCLUSION

In this report, I have tried to show some of the versatile capabilities of the small deposition chamber as a DC arc system for the study of plasma during the processing of nanostructures. Multiwalled carbon nanotubes are successfully synthesized by this experimental setup. The excitation temperature and the density within the plasma are successfully calculated the Boltzmann plots and the Saha-Eggert relationship respectively. I have modified the system to control the temperature using water cooling and a thermostat to enhance its performance for a variety of depositions. This system is very flexible that allows deposition of various materials with a very less mechanical job and in very short span of time (within 30 minutes if working at room temperature). The viewing window is positioned vertically to the plasma column, making the setup very appropriate to scan the plasma for spectroscopic studies. In conclusion, such setup is very useful to find quick results as far as research is concerned.

REFERENCES

1. Iijima S. Single-shell carbon nanotubes of 1 nm diameter. *Nature*. 1993;363:603-605.
2. Bethune DS, et al. Cobalt-catalysed growth of carbon nanotubes with single-atomic-layer walls. *Nature*. 1993;363:605.
3. Krätschmer W, et al. Solid C60: A new form of carbon. *Nature*. 1990;347:354.
4. Saito Y, et al. Yield of fullerenes generated by contact arc method under He and Ar: Dependence on gas pressure. *Chem Phys Lett*. 1992; 200: 643-648.
5. Collins PG. Nanotubes for electronics. *Scientific American*. 2000;283:62-69.
6. Li B. Discussion on emission spectroscopy measurements from a dense electrothermal launcher plasma. In *Proceedings of the 19th Int Symp Ballistics 2001*;5: 203.
7. Mohamed A, et al. Tribological behavior of carbon nanotubes as an additive on lithium grease. *Journal of Tribology*.2015;137:011801.
8. Pirlot C, et al. Preparation and characterization of carbon nanotube/polyacrylonitrile composites. *Adv Eng Mater*. 2002; 4: 109-114.
9. Endo M. Stacking nature of graphene layers in carbon nanotubes and nanofibres. *J Phys Chem Solids*. 1997;58:1707-1712.
10. Boncel S, et al. En route to controlled catalytic CVD synthesis of densely packed and vertically aligned nitrogen-doped carbon nanotube arrays. *Beil J Nanotech*. 2014;5:219.
11. Liu G, et al. Coulomb explosion: A novel approach to separate single-walled carbon nanotubes from their bundle. *Nano letters*.2008; 9:239-244.
12. Gupta VK. Carbon nanotubes-from research to applications. *Syntheses of carbon nanotube-metal oxides composites; adsorption and photogradation*. *InTech*. 2011;295-312.

13. Dobrzański L A, et al. Synthesis and characterization of carbon nanotubes decorated with platinum nanoparticles. *J Achie Mater Manu Engin.*2010;39:184-189.
14. S. S. Harilal, et al. Electron density and temperature measurements in a laser produced carbon plasma. *J. Appl Phys.* 1997;82:2140.
15. Banerjee S, et al. Molecular simulation of the carbon nanotube growth mode during catalytic synthesis. *App Phy Lett.* 2008;92:233121.
16. Encyclopedia Britannica, Nucleation, crystallography. Retrieved from the Encyclopedia Britannica website. 2014:21.
17. Guo T. Self-assembly of tubular fullerenes. *J Phys Chem.* 1995;99:10694-1069.
18. Inami, et al. Synthesis-condition dependence of carbon nanotube growth by alcohol catalytic chemical vapor deposition method. *Sci Technol Adv Mater.* 2007;8:292.
19. Ishigami N, et al. Crystal plane dependent growth of aligned single-walled carbon nanotubes on sapphire. *Journal of the American Chemical Society.*2008;130: 9918-9924.
20. Jeong HJ, et al. Narrow diameter distribution of singlewalled carbon nanotubes grown on Ni-MgO by thermal chemical vapor deposition. *Chem Phys Lett.* 2003;380:263-268.
21. Kónya Z, et al. XPS study of multiwall carbon nanotube synthesis on Ni-, V-, and Ni, V-ZSM-5 catalysts. *Applied Catalysis A: General.* 2004;260:55-61
22. Maruyama S, et al. Synthesis of single-walled carbon nanotubes with narrow diameter-distribution from fullerene. *Chemical Physics Letters.* 2003;375:553-559.
23. Karkhanis SN, et al. Natural graphite from Neoproterozoic psammitic gneiss, Inanalo Mountain, southern Madagascar. *Tectonophysics.* 2006;280:15-29.
24. Ren ZF, et al. Synthesis of large arrays of well-aligned carbon nanotubes on glass. *Science.* 1998;282: 1105-1107.
25. Iijima s. Helical microtubules of graphitic carbon. *Nature.* 1991;354:56-58.
26. SEM images and TEM images of carbon nanotubes, aligned carbon nanotube arrays, and nanoparticles. *Nano-lab.com.* 2012;6:6.